Representing Flow Patterns by Using Streamlines with Glyphs

David H.F. Pilar and Colin Ware

Abstract—Most professional wind visualizations show wind speed and direction using a glyph called a wind barb in a grid pattern. Research into flow visualization has suggested that streamlines better represent flow patterns but these methods lack a key property—unlike the wind barb, they do not accurately convey the wind speed. With the goal of improving the perception of wind patterns, and at least equaling the quantitative quality of wind barbs, we designed two variations on the wind barb and designed a new quantitative glyph. All of our new designs space glyph elements along equally spaced streamlines. To evaluate these designs, we used a North American mesoscale forecast model. We tested the ability of subjects to determine direction and speed using two different densities each of three new designs as well as the classic wind barb. A second experiment evaluated how effectively each of the designs represented wind patterns. The results showed that the new design is superior to the classic, but they also showed that the classic barb can be redesigned and substantially improved. We suggest that flow patterns with integrated glyphs may have widespread application in flow visualization.

Index Terms—Streamline placement, wind barb, glyph, flow visualization, weather maps, multivariate visualization

1 Introduction

Modern weather visualizations normally indicate wind speed and direction using a glyph called a *wind barb* [13]. The basic wind barb design has a shaft oriented in the wind direction and a set of bars and/or pennants to encode speed in 5 knot intervals (Fig. 1). Each half bar encodes 5 knots, and each full bar encodes 10 knots. The triangular pennant encodes 50 knots. The direction of the wind is from the tail (the part with the bars and pennants codes) to the tip. In weather displays (e.g., Fig. 2), wind barbs are either drawn on a regular grid or at the locations of wind measurement stations with the measurement location given by the position of the barb tip.

The 5 knot code of the wind barb means that they can be read to an accuracy of $+/-2.5$ knots. The speed code is easy to read and to learn, and wind barbs are a standard feature of meteorological maps. However, a previous study of modeled hurricane data by Martin et al. [5] showed that wind barbs lead to substantial errors in area wind speed estimation and also produce systematic biases in the perception of wind orientation. In the following discussion, we argue that wind barbs have several design features that interfere with the representation of wind direction and regional wind patterns. The problem may be especially acute in portrayals of computational weather models that generate dense continuous vector fields.

In the present paper, we report on an effort to develop a method for representing wind data that combines the virtues of the wind barb in the representation of quantity with the virtues of flow visualization methods that better show overall wind patterns for representing model output. Our goal is the effective portrayal of the dense wind patterns that are generated by operational wind forecast models. Our solution, we believe, can have widespread application in flow visualization.

We begin with an analysis of the strengths and weaknesses of wind barbs as well as alternative methods that have been developed to represent flow patterns. We organize our analysis around a breakdown of the components of a two-dimensional (2D) vector. Vectors are often defined in terms of two components: direction and magnitude. For the purposes of analyzing the effectiveness of flow visualization, it is useful to break the concept down even further, separating direction into two parts, orientation and direction sign [11]. The orientation is simply the angle as expressed by a line segment, and the direction sign differentiates the two ends of that line segment. A streamline trace, for example, shows orientation at every point along its length, but no direction sign. Arrowheads are one method for encoding direction sign.

1.1 Orientation

With a wind barb, the shaft orientation indicates wind orientation at the tip location. There are a number of perceptual problems with this. First, untrained observers may judge wind orientation to occur in the middle of the barb, or at some other point, perhaps even the tail where the visual weight is greatest. Second, the bars and pennants create their own orientation pattern at approximately 45 degree angles to the flow. Having the measurement location at the tip may be responsible for the systematic orientation errors recorded by Martin et al. [5]. Bars also introduce sharp changes in contour direction that break continuity and make it difficult to identify patterns such as wind fronts or cyclones. Third, wind patterns curve continuously but because of its long straight shaft, only a very small part of the wind barb contour is actually aligned with the wind direction, and this point is far from the visual center of the glyph.

• *The authors are with the Center for Coastal and Ocean Mapping, University of New Hampshire, Durham, NH 03824. E-mail: {cware, dpilar}@ccom.unh.edu.*

Manuscript received 6 Jan. 2012; revised 26 July 2012; accepted 19 Dec. 2012; published online 23 Jan. 2013.
Recommended for acceptance by R. Machiraju.
For information on obtaining reprints of this article, please send e-mail to: tvcg@computer.org, and reference IEEECS Log Number TVCG-2012-01-0006.
Digital Object Identifier no. 10.1109/TVCG.2013.10.

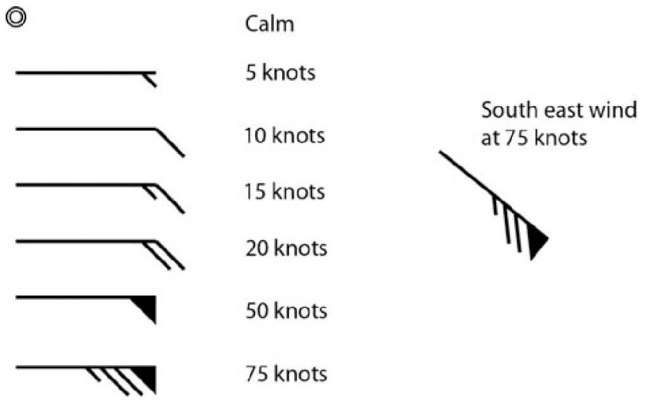

Fig. 1. The wind barb glyph code use in meteorological maps.

Streamlines are well suited for showing vector field orientation [4], [6], [10], and there are efficient algorithms that enable equally spaced streamlines to be constructed [4], [7]. A number of authors have proposed that directional glyphs should be drawn head-to-toe, bent along the flow direction using streamlines to guide placement [4], [6]. Pineo and Ware [9] showed that this organization best stimulates contour detection mechanisms in the primary visual cortex and argued that this supports both the task of streamline tracing and the judgement of wind orientation at an arbitrary point on a map.

In an evaluation of six flow visualizations, Laidlaw et al. [6] found arrows drawn on a regular grid to be particularly poorly suited for judging advection pathways. Part of the problem is that the grid is itself a pattern that has no meaning with regard to the data. Fig. 2, for example, shows strong oblique patterns in the upper part of the map that have nothing to do with the flow direction. These patterns are artifacts of the grid, and they contain a stronger orientation signal than do the individual wind barbs that make up the pattern. Shifting or jittering the grid has been shown to alleviate the problem of false pattern to some degree [6].

1.2 Direction Sign

Bertin [1] suggested that arrows are effective because they contain a greater weight at the head, and Ware [11] argued that a perceptual mechanism supporting this may be found in end-stopped neurons of the primary visual cortex. The wind barb, however, has its greatest visual weight at the tail of the barb and may be confusing to the nonexpert for this reason.

1.3 Magnitude

To show wind speed effectively, a method is required that maps wind speed to some monotonically increasing visual attribute, such as line width or line weight [12]. Wind barbs achieve this to some extent, because barbs representing stronger winds tend to have more bars or pennants, increasing their visual weight. Nevertheless, many of the methods developed by the visualization community are far better at representing the pattern of wind speeds, for example, by varying the line weight, the degree of contrast, or the glyph size [1], [2], [3], [8]. Another method for showing wind speed is to use the background color to encode wind speed, which can be effective if it is done using a perceptually monotonically increasing scale [13]. Still, color coding speed is not always possible, because color may be needed to show some other scalar variable, such as surface temperature.

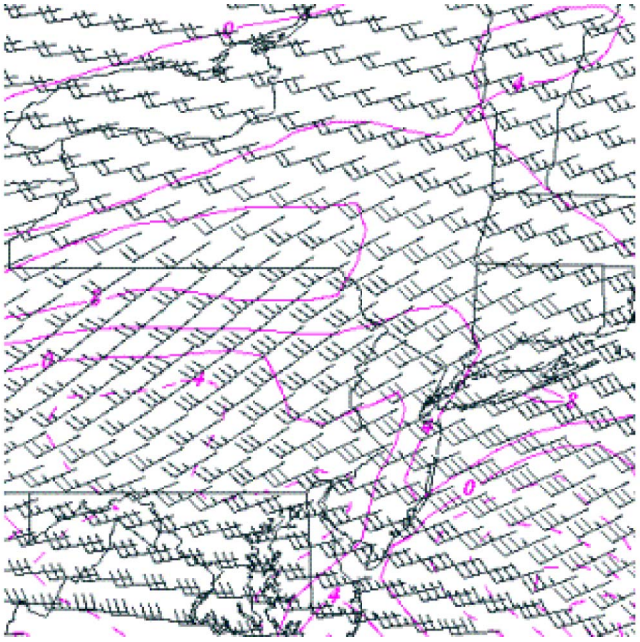

Fig. 2. The output from a wind forecast model obtained from a NOAA website: http://www.erh.noaa.gov/bgm/casestudy/2002/jan19/Jan19_files/image034.gif.

The greatest strength of the wind barb, and presumably the reason why it is so widely used, is that it is quantitative in a way that most visualization techniques are not. Arrow length, glyph size, linewidth, and other smoothly varying visual attributes used to convey speed all suffer from the same perceptual problem, namely simultaneous contrast [12]. The visual system is very good at judging *relative* size, color, or texture density, but it is very poor at judging *absolute* size, color, or density; these properties are altered by contrast with surrounding elements, and this can lead to systematic errors [12].

Our study had both a design phase and an evaluation phase. In the design phase, we evolved a series of new designs, each of which incorporated some change that improved on the previous one. We took advantage of design principles suggested by previous work.

2 Design

We started with the assumption that it should be possible to create a method that combines the virtues of wind barbs in encoding a clearly readable wind speed, with the virtues of streamlines in encoding orientation and showing the wind patterns.

Our design goals were as follows:

1. Create a coding that, like the classic wind barb, enables wind speeds to be read with an accuracy of $+/-2.5$ knots.
2. Make the wind orientation and direction patterns as clear as possible.
3. Make the wind speed pattern as clear as possible: Ideally, the viewer should see at a glance where the areas of high and low wind speeds are located.
4. Show as much wind pattern detail as possible.

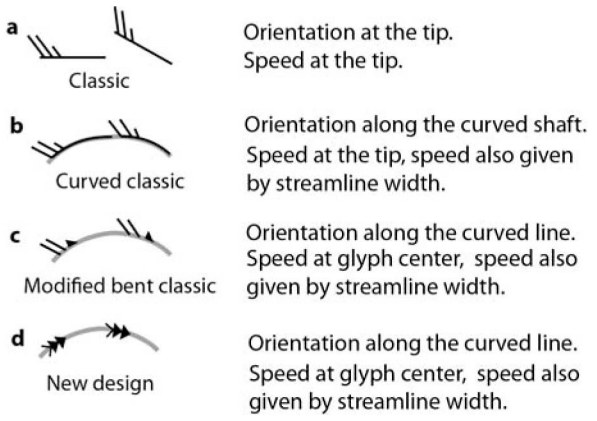

Fig. 3. The four designs that we evaluated. (a) The classic wind barb. (b) The classic with a curved shaft. (c) Modified classic on a streamline. (d) The new arrow glyph design on a streamline.

We carried out a staged approach to the redesign. First, we were interested in seeing if the classic barb could be redesigned to show the wind patterns better.

2.1 Design 1: Classic

For comparison with our new designs, we also implemented a design consisting of a grid of traditional wind barbs. The density of the glyphs was the same as the density of the glyphs in the other designs.

2.2 Design 2: Curved, Aligned Wind Barbs

Since wind barbs are so well established in wind visualization, we explored designs that retained the basic coding scheme. The design has the following features:

- The shaft of the barb is curved so that it conforms to a streamline.
- Curved barbs are placed head-to-tail along an extended streamline created using the Jobard and Lefer algorithm [4].
- The width of the line making the streamline is increased according to wind speed, resulting in greater visual density where wind speeds are stronger.
- Dotted lines are drawn for speeds less than 7.5 knots.

This design is illustrated in Figs. 3b, 4b, and 5b. For these barbs, the point of speed measurement is at the head as it is for the classic barb.

2.3 Design 3: Modified Barb Coding on Streamlines

The second design makes somewhat greater modifications to the standard wind barb:

- The shaft of the barb is eliminated.
- The bars and pennants are arranged along continuous streamlines generated using the Jobard and

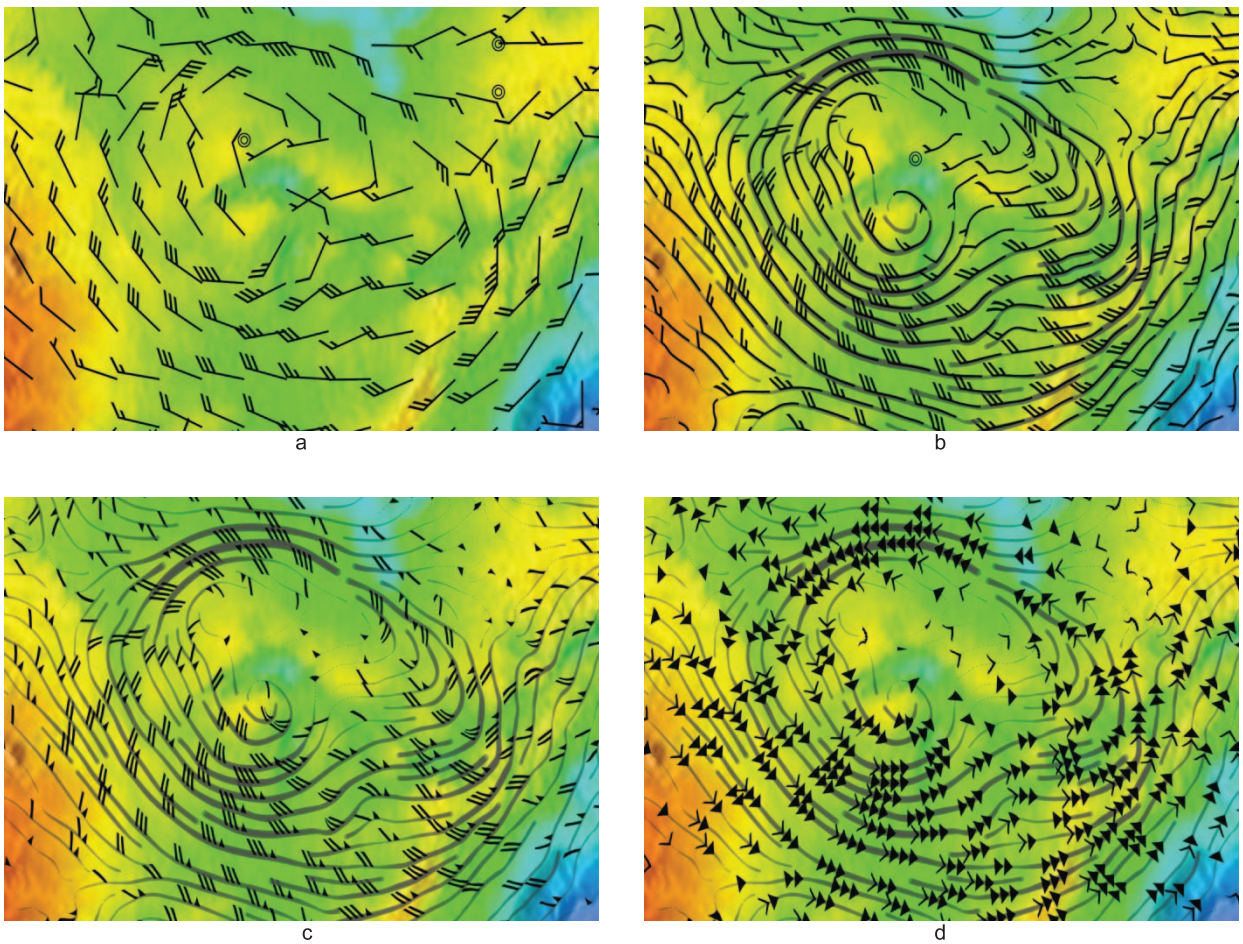

Fig. 4. Low density representations from top: (a) The classic wind barb drawn on a grid. (b) The classic with a curved shaft. (c) Modified classic on a streamline. (d) The new arrow glyph design on a streamline.

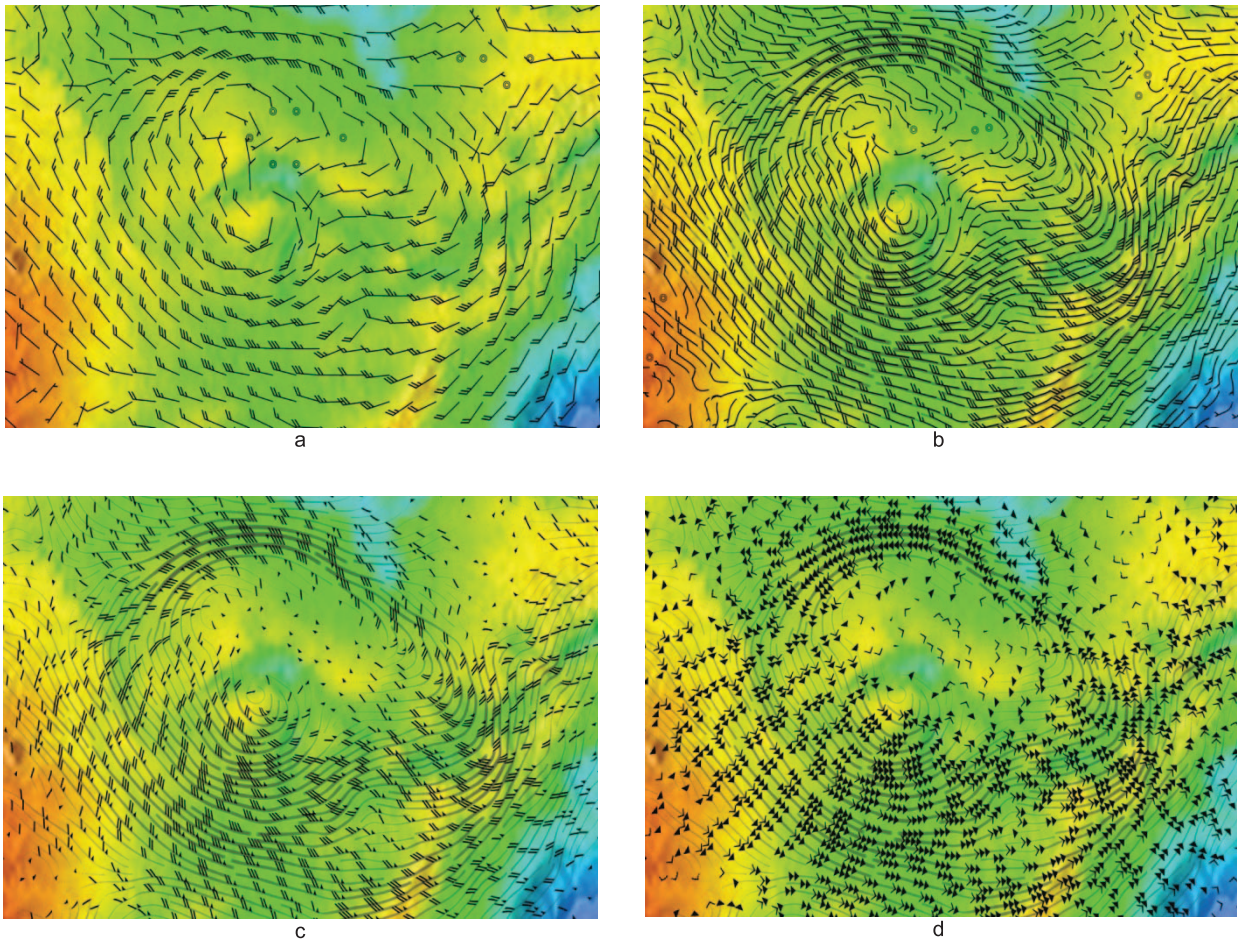

Fig. 5. High density representations from top: (a) The classic wind barb drawn on a grid. (b) The classic with a curved shaft. (c) Modified classic on a streamline. (d) The new arrow glyph design on a streamline.

Lefer algorithm [4]. Wind speeds are represented on the contour at the location of the bars and pennants.

- A small triangle is used to represent 5 knots instead of the short bar. The short (5 knot) bar of the speed code can sometimes be confused with the longer (10 knot) bar; however, the size differential between the 5 and 50 knot triangles is greater than the size differential between the 5 and 10 knot bars so the two are less likely to be confused.
- The width of the line making the streamline is increased according to wind speed, resulting in greater visual density where wind speeds are stronger.
- Dotted lines are drawn for speeds less than 7.5 knots

This design is illustrated in Figs. 3c, 4c, and 5c.

2.4 Design 4: New Arrow Glyphs on Streamlines

The third design is a much more radical departure from the classic barb. It retains the coding in 5 knot units but uses a different symbology:

- The coding, like wind barbs, has design elements for 5, 10, and 50 knots. It is illustrated in Fig. 6.
- Symmetrical arrow heads are used. This is intended to reduce the visual aliasing effects that can arise with the classic barb. It also is designed to allow for closer placement of streamlines.
- The arrow glyphs are arranged along a continuous streamline generated using the Jobard and Lefer algorithm [4]. Also, the quantity that is represented is at the center of the glyph.
- The width of the line making the streamline is increased according to wind speed, resulting in greater visual density where wind speeds are stronger.
- Dotted lines are drawn for speeds less than 7.5 knots.

This design is illustrated in Figs. 3d, 4d, and 5d.

3 Implementation

The Jobard and Lefer [4] algorithm was chosen to calculate equally spaced streamlines for all of the new designs because of its computational speed and simplicity. The glyphs were drawn along the streamlines using predrawn texture images, one for each 5 knot interval. This made it

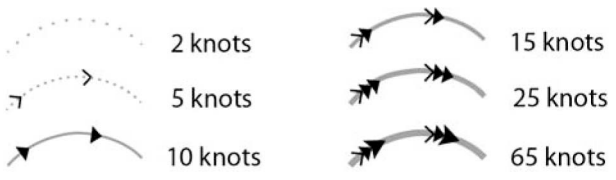

Fig. 6. The new arrow glyph code.

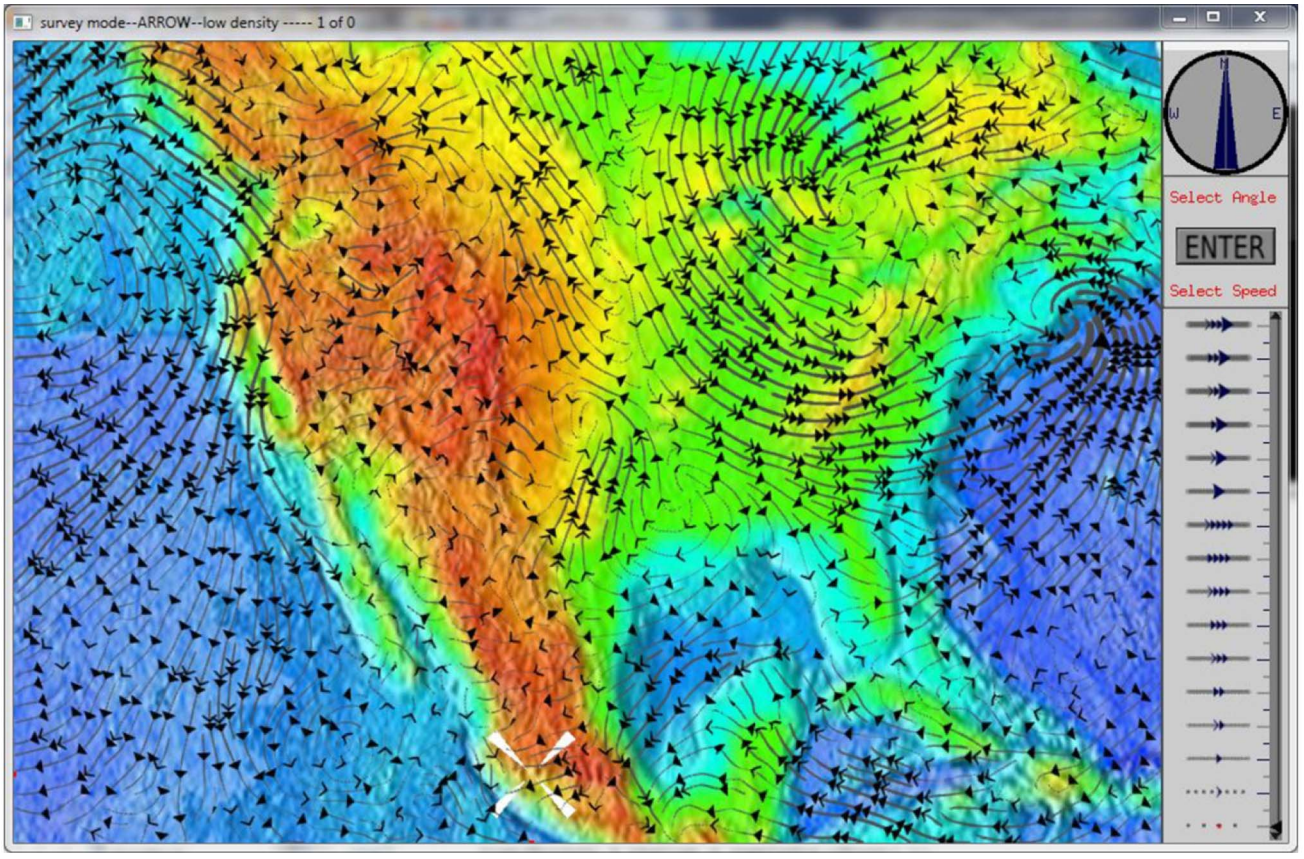

Fig. 7. The display used for the experiment. The participant rotated the compass arrow at the top right to indicated direction and the scale below to indicate speed at the center of the white cross.

possible to change the glyph design simply by changing the texture images. The images were antialiased and interpolated mipmaps were used in rendering.

The model data used to evaluate the different representations came from the NOAA National Centers for Environmental Prediction (NCEP) North American Mesoscale forecast model. Three different forecasts were used to provide variation in wind patterns and speed fluctuation. The forecasts used were downloaded from *ftpprd.ncep.noaa.gov/pub/data/nccf/com/nam/prod/* for the following dates and times: 7/13/2010 00:00:00 UTC at time index 26; 7/26/2010 00:00:00 UTC at time index 11; and 9/2/2010 12:00:00 at time index 18.

To evaluate how well the different designs could accommodate higher densities of information, we implemented each design with two different line spacings, and with glyph sizes scaled accordingly. The detailed parameter settings were as follows:

The parameter used to control line spacing in the Jobard and Lefer algorithm is Dsep. This was set to 5 pixels for the small styles, and 9 pixels for the large styles. Dtest, the minimum allowable distance between streamlines, was 0.75 * Dsep. In practice, this resulted in streamlines with spacings between 3.75 and 7.5 pixels. There were 37.59 pixels/cm. The result is 1-2-mm line spacing for the small styles and 1.5-3-mm line spacing for the larger styles.

The width of the classic, curved classic, and modified classic was 0.133 mm for small and 0.239 mm for large. The length of the classic and curved classic shafts was 0.452 cm for small and 0.771 cm for large. The modified classic and the new arrow glyph were spaced along the streamline at 0.532 cm for small and 0.958 cm for large. The width of the triangles that represent the value 10 for the new arrow glyph was 0.133 mm for small and 0.239 mm for large.

Line width was determined using the formula:

$$width = 0.5 + \frac{speed}{12},$$

where *width* is in pixels and *speed* is in knots. Streamline sections where speeds were less than 8 knots were drawn as dotted lines according to the algorithm:

$$if\ speed\ < 4, sp = 6 - speed$$
$$else\ if\ speed < 6, sp = 2$$
$$else\ if\ speed < 8, sp = 1,$$

where *sp* is spacing in pixels.

The window was 27.5 cm wide $\times$ 18 cm high with a wind field of 24.5 cm $\times$ 17.1 cm. See Fig. 7.

A colored background image consisting of a map of North America was used because the designs are intended to allow for a color-coded background. There was no functional significance beyond providing context and a variety of colors.

4 Evaluation

We carried out two separate evaluation experiments. The first was an evaluation of how well the different methods portrayed wind speed and direction. The second was an

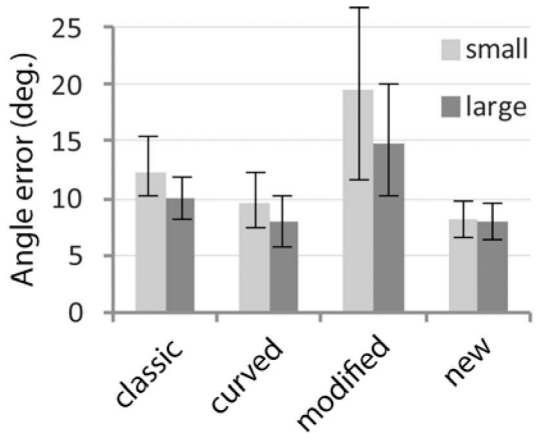

Fig. 8. Average angle error for the different designs. Bars represent two standard errors.

evaluation of how the different designs portrayed detailed pattern information.

4.1 Experiment 1

Speed and direction judgements: The first experiment used the NCEP forecast model data as a basis for creating the wind patterns. For each of the designs, we measured the accuracy with which a subject could judge the wind speed and direction at points randomly selected from the map.

4.2 Tasks

On each trial, the subject was required to estimate wind speed and direction at a point on the map designated by a white cursor. The cursor consisted of four triangles converging on a single point at which the values were to be interpolated. Fig. 7 illustrates the screen.

To make a wind direction estimate, subjects used a widget resembling a compass with a needle in the upper right-hand corner. Clicking and dragging with the mouse altered the orientation of the needle. Subjects used a slider below the compass to enter their wind speed estimate measured in knots. Both widgets were primarily manipulated with a mouse, but could be "fine tuned" with the keyboard arrow keys. The keyboard enter button was used to finalize selections. Both selection widgets were initialized to zero, and both must have been used prior to the "enter" button being selected to progress to the next trial.

4.3 Conditions and Trials

The independent variables consisted of four different designs: classic barb, curved classic, modified classic, and new arrow glyph, each with two spacings yielding eight conditions.

For each condition, there were 18 trials: Three different sets of weather model data were used, and for each set, six different points were randomly selected.

The subject first completed a training session consisting of 16 trials, two each from the two different sizes of the four different styles. During training, subjects were provided with feedback for their selected measurements.

The experiment consisted of 144 trials, 6 each for each combination of 2 sizes $\times 4$ designs $\times 3$ forecasts. The trials were divided into 24 blocks of 6, where condition and forecast remained constant for the block. Latin squares

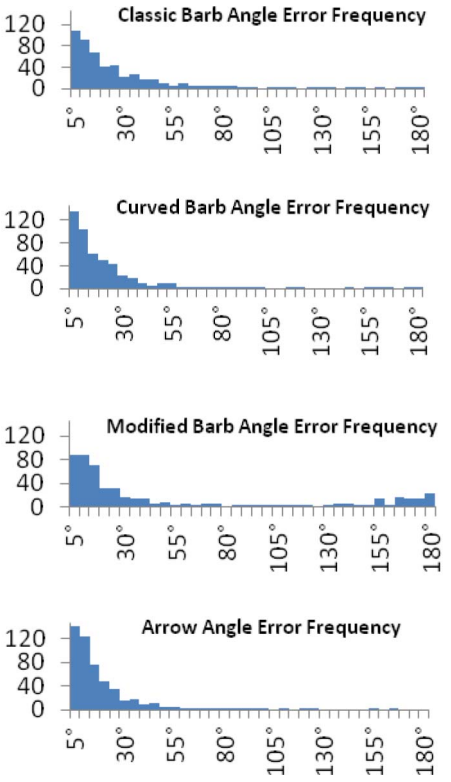

Fig. 9. The distributions of angular errors for the different designs.

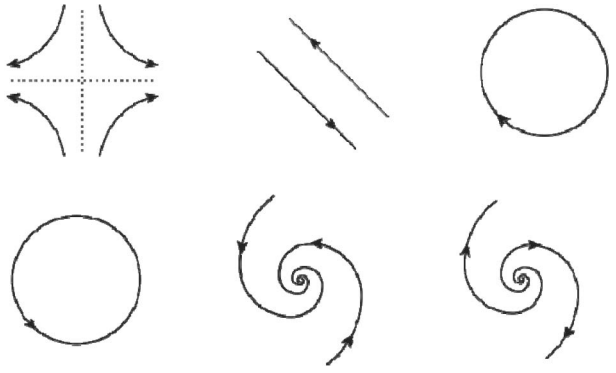

Fig. 10. The six patterns used as targets: (a) saddle, (b) shear, (c) clockwise circle, (d) counterclockwise circle, (e) spiral in, and (f) spiral out.

were used to ensure that no size-design combination was adjacent, and each subject was given a different random block order. Maps were randomly assigned to blocks, constrained so that each size-design combination appeared in one block for each map.

4.4 Participants

There were 13 participants, all undergraduate students who were paid for taking part.

4.5 Results from Experiment 1

Some irregularity in the data set occurred due to areas of very low wind speed (<5 knots), or in areas of turbulence, where direction may change rapidly over a small area. In such areas, all representations suffered from large angle errors because curved and streamline designs filter out tight spirals by design, and straight representations are too sparse to capture the pattern. We used the log of the errors in the ANOVAs to

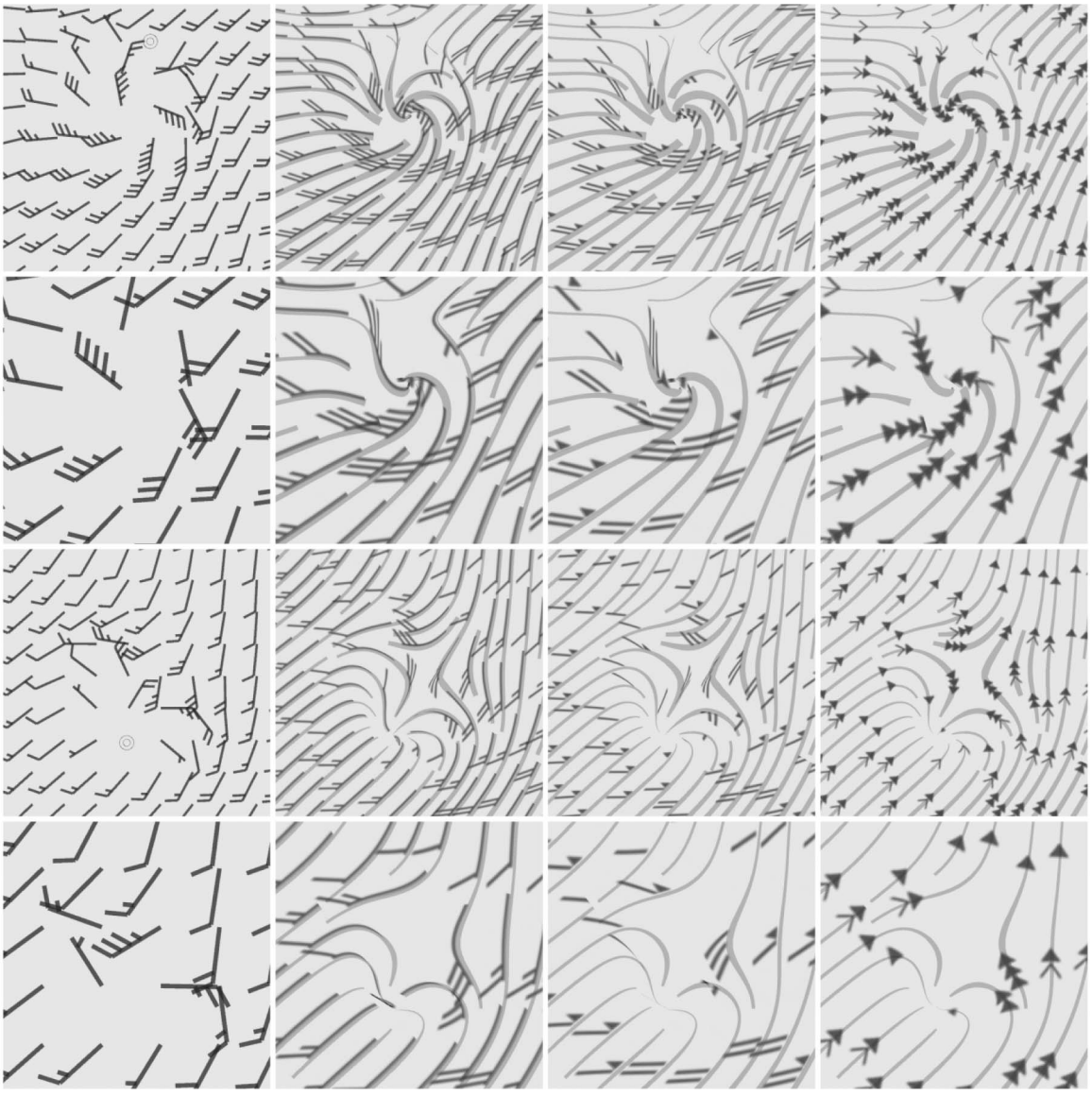

Fig. 11. Examples of two of the patterns used in the second experiment shown using the four designs. Top row inward spiral (small spacing). Second row: inward spiral (large spacing). Third row: saddle (small spacing). Fourth row: saddle (large spacing).

lessen the effect of these extreme errors on the results and to make the distribution of errors more nearly normal.

Fig. 8 shows the average angle error for the different designs. An ANOVA with Greenhouse-Geisser adjustments for violations of sphericity revealed a main effect for the different designs $(\mathrm{F}[3, 36] = 21.1;\ \mathrm{p} < 0.01)$ with an effect for the size $(\mathrm{F}[1, 12] = 8.0;\ \mathrm{p} < 0.02)$ and no interaction. A Tukey HSD test showed the arrow and curved classic designs to have the lowest error with no statistical difference between them. The classic design came next, and the modified design resulted in the greatest mean error.

To try to account for the failure of the modified design, we examined the distribution of angular errors. These results are shown in Fig. 9, and they show that for the modified barb design, there was a bimodal error distribution, approximately 17 percent of the results were at 180 degrees to the true direction. The number of 180 deg errors was negligible for the other conditions.

Statistically, all of the designs were equally good at representing wind speed. An ANOVA revealed no effects for either size or design. The overall average speed error was 1.95 knots.

4.6 Experiment 2: Patterns

We carried out a second experiment to evaluate the different designs in terms of how well they convey pattern information. For each trial of this experiment, we generated a new artificial flow field where one of six artificial patterns had been embedded.

4.7 Display

An artificial flow field was generated by randomly summing 2D gabor functions, into a 2D array. This was done independently for the u and v velocity vectors to produce a smoothly varying pseudorandom flow field. As a final step, generation of a constant vector was added so that the overall trend was always from the lower left to the upper right. This was done to avoid the random generation of patterns corresponding to the targets the subjects were expected to locate.

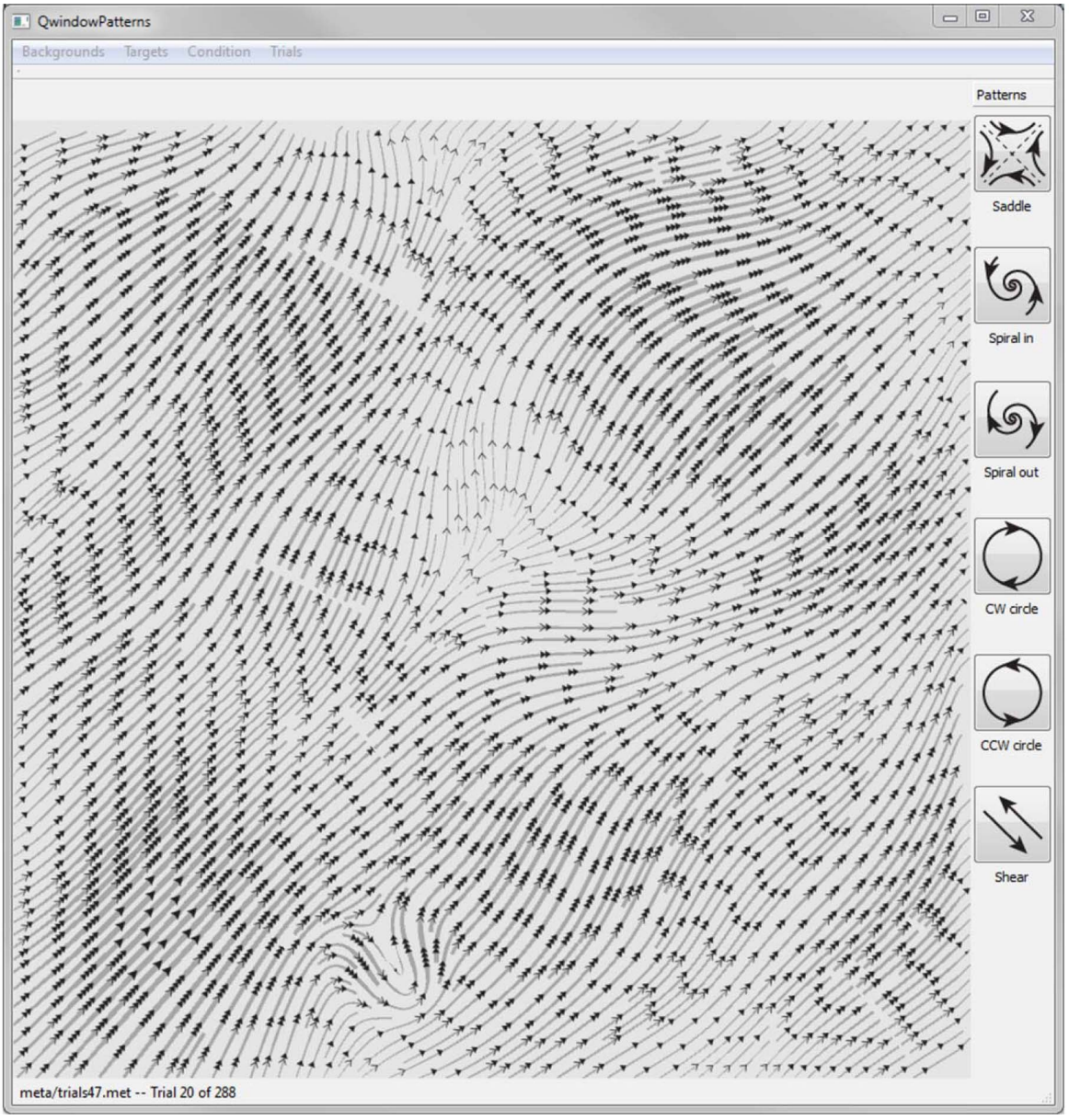

Fig. 12. The screen the subject saw for Experiment 2.

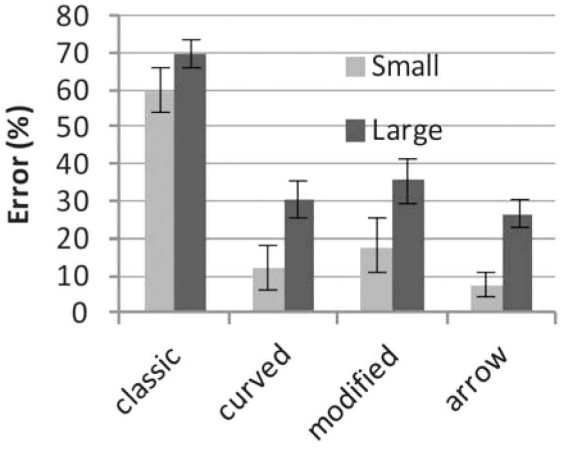

Fig. 13. Mean errors for Experiment 2 pattern task.

On each trial, a different target pattern was added to the random flow field using a Gaussian blending function. The set of target patterns was made up of a saddle, a shear, clockwise, and counterclockwise circulation patterns, as well as an inward and an outward spiral. The set is illustrated in Fig. 10.

Examples of two of the patterns as they were rendered by the four designs are given in Fig. 11.

4.8 Conditions and Trials

The independent variables consisted of four different designs: classic barb, curved classic, modified classic, and new arrow glyph, each with two spacings yielding eight conditions. For each condition, there were 36 trials: Six different patterns were used, and for each, there were six replications. New random flow fields were generated for every trial.

The subject first was introduced to the four different glyph designs, and then completed a training session

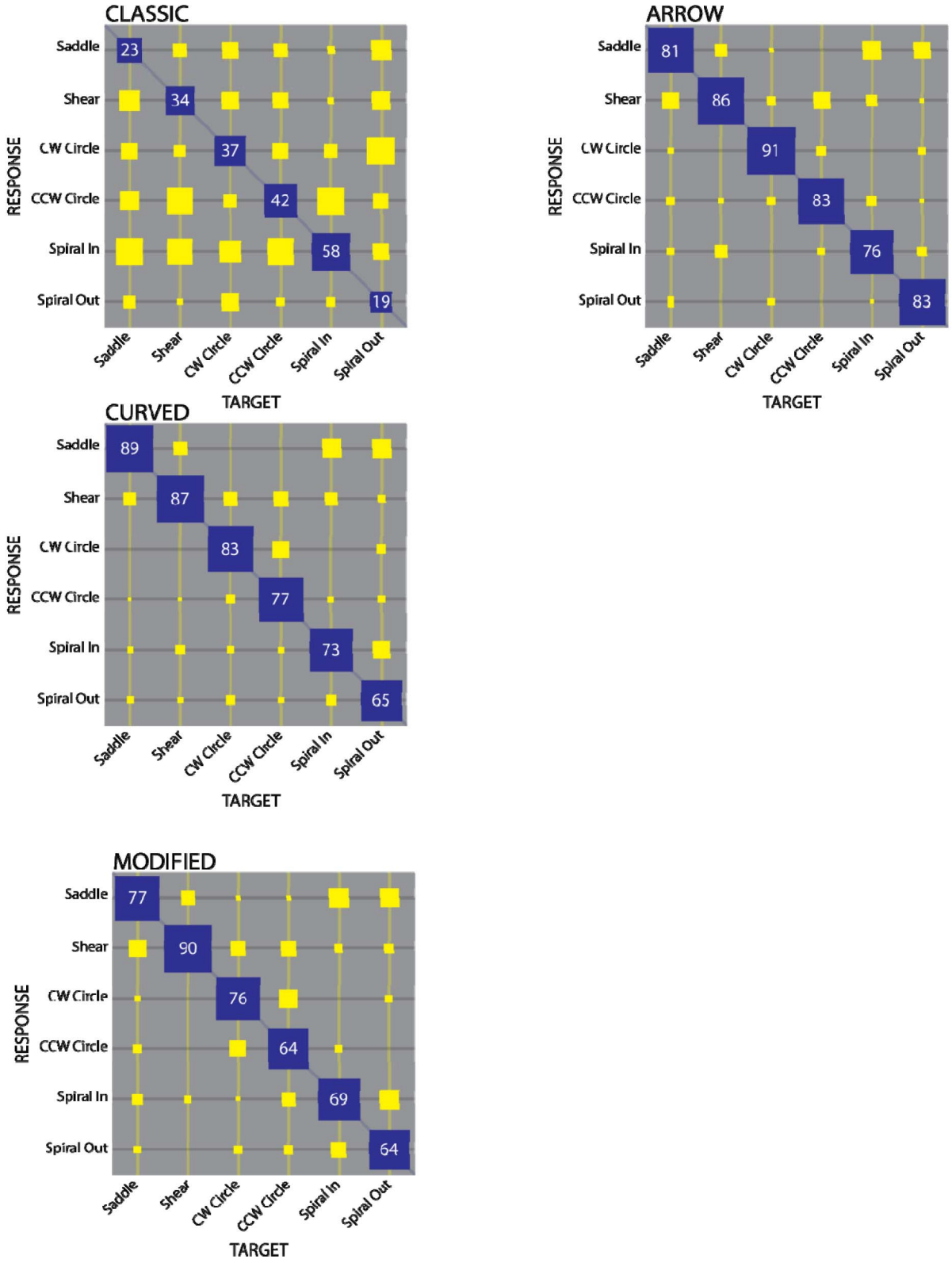

Fig. 14. Experiment 2 detailed results. Each chart shows the confusion matrix for a single design. The pattern displayed is given on the x-axis; the response is on the y-axis. The size of each square is proportional to the number of response. Blue squares are correct responses. (a) The classic wind barb drawn on a grid. (b) The classic with a curved shaft. (c) Modified classic on a streamline. (d) The new arrow glyph design on a streamline.

consisting of 48 trials, one for each combination of four designs with two sizes each and six patterns. The subjects were not limited in time for the training session and were provided with feedback for their selected patterns.

The experiment consisted of 288 trials, 6 for each combination of 2 sizes $\times 4$ styles $\times 6$ patterns. The trials were divided into 24 blocks of 12 with the option for a break after every two blocks. Size and design remained constant

within a block, but the target patterns were randomly distributed across all the trials in a way that ensured all conditions used each target pattern exactly six times.

4.9 Task

The task was a six alternative forced choice. On each trial, the subject was given a 4 second exposure to a flow field containing one pattern. To enter their choice, subjects clicked on one of the six buttons to the right of the screen. See Fig. 12.

4.10 Participants

There were 11 participants: two undergraduate students, five visLab employees, and four others. Four were female.

4.11 Results from Experiment 2

Fig. 13 shows the mean errors for each design. A two-way ANOVA with Greenhouse-Geisser adjustments for violations of sphericity revealed a main effect for the different designs $(F[1, 10] = 86;\ p < 0.01)$ with an effect for the size $(F[1, 10] = 115.9.0;\ p < 0.01)$ and no interaction. A Tukey HSD test revealed the classic design to be worse than all of the others. The curved barb and the arrow designs were tied as best with the modified design worse than the arrow design but not significantly different from the curved design.

The pattern of errors is summarized in Fig. 14 with a set of error matrices. An angular bias for circular pattern is evident in the classic design. The most common error for counterclockwise circle was a counterclockwise spiral in. This can be explained if the orientation is judged at some point on the shaft of the barb instead of just at the tip. The fact that a spiral out was most frequently judged to be a counterclockwise circle can be explained in the same way. For the other designs, the most systematic bias was a tendency to see spirals as saddles.

5 Discussion

Overall, the results show that combining a quantitative glyph with continuous streamlines to show patterns is a successful strategy. Two of our new designs turned out to be measurably better than wind barbs in terms of the accuracy with which wind speed and orientation can be read. Our second redesign (the modified barb) was less successful, producing the largest angle errors. In this case, the bimodal distribution of errors suggests that direction sign may be ambiguous (sometimes, the speed lines could completely span the gap between the streamlines) resulting in the 180 degree errors. It should be noted that the modified barb lacked the additional direction-sign cue provided by the shaft in the curved and classic designs.

All of our new streamline-based designs were greatly superior to the grid of classic wind barbs in their ability to represent the detailed patterns shown in our second experiment, and this has practical implications. For applications where it is important that the traditional wind barb coding be retained, we suggest placing wind barb symbols along streamlines and curving the shaft of the barb to conform to the streamlines. In addition, streamline thickness should be increased with wind speed to make it easier to distinguish high wind from low wind areas. This will enable meteorologists to continue to use the familiar speed coding of the wind barb, while gaining the advantage of superior pattern portrayal.

Our new design, based on arrow glyphs, is capable of better revealing the details of complex wind patterns: In the pattern task, it produced about 25 percent of the number of errors compared to the grid of wind barbs.

The ideas in this paper have even broader applications and may be useful in any case where there is a need to accurately represent both vector magnitude and the vector pattern of a flow field; for example, they might be used in the representation of ocean currents. To stretch the idea further, we are currently developing ways of using streamlines integrated with a quantitative glyph system to represent the output of computational models of ocean waves, and we are making the streamlines orthogonal to the direction of wave propagation so that they resemble wave fronts; the glyphs have been redesigned to show wave height. In general, the glyph plus streamline technique is most applicable when flow patterns must be combined with the representation of an additional scalar field such as temperature normally represented using a color sequence, making color coding unavailable to represent speed.

Acknowledgments

The authors wish to thank John Kelly, for advice on matters meteorological and Matt Plumlee for coding assistance. Olivia McGlone did an excellent job of running the participants though the study. This work was supported by NOAA Grant # NA05NOS4001153 and partially fulfilled the requirements for the MS degree in computer science at the University of New Hampshire.

References

[1] J. Bertin, *Semiology of Graphics.* Univ. of Wisconsin Press, 1983.
[2] D. Fowler and C. Ware, "Strokes for Representing Univariate Vector Field Maps," *Proc. Graphics Interface,* pp. 249-253, 1989.
[3] C.G. Healey and J.T. Enns, "Large Datasets at a Glance: Combining Textures and Colors in Scientific Visualization," *IEEE Trans. Visualization and Computer Graphics,* vol. 5, no. 2, pp. 145-167, Apr.-June 1999.
[4] G. Jobard and W. Lefer, "Creating Evenly-Spaced Streamlines of Arbitrary Density," *Proc. Eurographics Workshop Visualization in Scientific Computing,* pp. 45-55, 1997.
[5] J.P. Martin, J.E. Swan, R.J. Moorhead, Z. Liu, and S. Cai, "Results of a User Study 2D Hurricane Visualization," *Proc. 10th Joint Eurographics/IEEE-VGTC Conf. Visualization (EuroVis),* vol. 27, no. 3, pp. 991-998, 2008.
[6] D. Laidlaw et al., "Comparing 2D Vector Field Visualization Methods: A User Study," *IEEE Trans. Visualization and Computer Graphics,* vol. 11, no. 1, pp. 59-70, Jan./Feb. 2005.
[7] Z. Lui, R. Moorhead, and J. Groner, "An Advanced Evenly Spaced Streamline Placement Algorithm," *IEEE Trans. Visualization and Computer Graphics,* vol. 12, no. 5, pp. 965-972, Sep./Oct. 2006.
[8] P. Mitchell, C. Ware, and J. Kelley, "Designing Flow Visualizations for Oceanography and Meteorology Using Interactive Design Space Hill Climbing," *Proc. IEEE Int'l Conf. Systems, Man and Cybernetics,* pp. 355-361, 2009.
[9] D. Pineo and C. Ware, "Neural Modeling of Flow Rendering Effectiveness," *ACM Trans. Applied Perception,* vol. 7, no. 3, pp. 1-14, 2010.
[10] G. Turk and D. Banks, "Image-Guided Streamline Placement," *Proc. ACM SIGGRAPH,* vol. 96, pp. 453-460, 1996.
[11] C. Ware, "Towards a Perceptual Theory of Flow Visualization," *IEE Computer Graphics and Applications,* vol. 28, no. 2, pp. 6-11, 2008.

[12] C. Ware, *Information Visualization Perception for Design*, second ed. Morgan Kaufman, 2004.
[13] C. Ware, "Color Sequences for Univariate Maps: Theory, Experiments and Principles," *IEEE Computer Graphics and Applications*, vol. 8, no. 5, pp. 41-49, Sept. 1988.
[14] Wikipedia, "Station Model,"http://en.wikipedia.org/wiki/Wind_barb#Plotted_winds.W.-K., Dec. 2009.

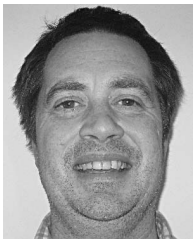

David H.F. Pilar received the BA degree in english and the MS degree in computer science from the University of New Hampshire. He is currently a research assistant for the Data Visualization Research Laboratory in the Center for Coastal and Ocean Mapping.

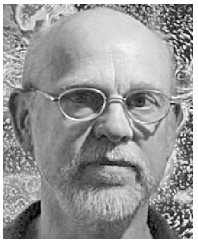

Colin Ware received the PhD degree in experimental psychology from the University of Toronto and the MMath degree in computer science from the University of Waterloo. Since 2000, he has been a professor of computer science and the director of the Data Visualization Research Laboratory in the Center for Coastal and Ocean Mapping at the University of New Hampshire. His research interests include the application of perceptual principles to data visualizations and the design of interactive data displays. He is the author of *Information Visualization: Perception for Design*, and more than 150 articles in journals and refereed conference proceedings.